International Journal of Geographical Information Science
Vol. 20, No. 1, January 2006, 103–115

Taylor & Francis
Taylor & Francis Group

Research Article

First evidence of West Nile virus amplification and relationship to human infections

C. N. THEOPHILIDES*†, S. C. AHEARN†, E. S. BINKOWSKI‡, W. S. PAUL§ and K. GIBBS§

†Center for Advance Research of Spatial Information, Hunter College of The City University of New York, New York, NY 10021, USA

‡Department of Mathematics and Statistics, Hunter College of The City University of New York, New York, NY 10021, USA

§Epidemiology and Disease Control Programs, Chicago Department of Health, Chicago, IL 60604, USA

(*Received 16 March 2005; in final form 7 June 2005*)

The spatio-temporal relationship between unusual sightings of dead birds and human West Nile virus infections has been observed in many studies and has been proposed as an indicator of an intense amplification cycle between birds and mosquitoes. However, to date, no single study has provided quantitative evidence that the amplification cycle occurs at the local level and that it operates within certain temporal parameters. Here, we use a novel geostatistical and spatial analytic methodology and present the first evidence that the localized unusual space–time correspondence of dead birds models the amplification cycle and that this cycle peaks 15–16 days prior to human onset of West Nile virus infections. During the process of establishing this relationship, we extend the traditional Knox space–time interaction measure to overcome pair-dependency limitations and use a novel implementation of the kappa non-chance agreement measure to identify the temporal characteristics of the association of bird deaths to human West Nile infections.

Keywords: West Nile virus; Space–time clustering; Knox test; Monte Carlo; Kappa statistic

1. Introduction

The West Nile virus (WNV) is a mosquito-borne disease-causing infectious agent that affects wildlife and domestic animals. It can occasionally cause fever and encephalitis in humans and, in rare cases, can be fatal. First isolated in the West Nile district of Uganda (Smithburn *et al.* 1940), it was considered to be enzootic (perennially circulating among the animal population) to the Middle East, Africa, and Eurasia (Hayes *et al.* 2001) until 1999. In 1999, it was identified for the first time in the Western Hemisphere (Lanciotti *et al.* 1999, Nash *et al.* 2001), and since then it has been causing seasonal epidemics infecting thousands of people and infecting a wide variety of species in great numbers, mostly birds.

*Corresponding author. Present address: 1023 HN, 695 Park AvenueNew York, NY 10021, USA. Email: ctheo@geo.hunter.cuny.edu

International Journal of Geographical Information Science
ISSN 1365-8816 print/ISSN 1362-3087 online
http://www.tandf.co.uk/journals
DOI: 10.1080/13658810500286968

Since its introduction to the Americas, the disease has received renewed attention by researchers. The limited knowledge of how the disease circulates in the naïve-American wildlife prompted research on two major fronts. One was research focused on laboratory experiments that investigated the biological potential of mosquitoes and birds to acquire and transmit the virus (i.e. Komar *et al*. 2003). The other major front of the research focused on investigating the field dynamics of West Nile virus transmission and the interaction of mosquitoes, birds, and animals that could result in West Nile virus amplification and human infections (i.e. Kulasekera *et al*. 2001).

Laboratory analysis found that the most competent reservoir hosts are resident passerine bird species, and mortality is higher in corvids (McLean *et al.* 2001, Komar *et al*. 2003). According to Komar *et al*. (2003), American crows develop the highest viremia (amount of virus circulating in their blood) in 4–5 days post-infection and on average die on day 5. The same study showed that their mortality rate was found to be 100%, and a study by Yaremych *et al*. (2004) has verified this high mortality of crows due to WNV in the wild. Blue jays develop highest viremia levels on days 1, 2, 3, and 4 post-infection and on average die 4.7 days post-infection at a 75% rate (Komar *et al*. 2003)

A significant part of field research relates to the identification of proxies for WNV presence in specific areas so that public-health officials could intervene with control measures (Eidson *et al*. 2001) and reduce the risk of infection in humans. These spatially oriented risk-determining models initially appeared with the measurement of spatial densities of dead crows (Eidson *et al*. 2001) that soon proved limited. Later, Mostashari *et al*. (2003) used spatial models that attempted to overcome the limitation of density measures by using a modified version of the SatScan statistic (Kulldorff 1997). Theophilides *et al*. (2003), building on ideas by Rogerson (2001), developed a localized dynamic implementation of the Knox (1964). Called the Dynamic Continuous Area Space–Time (DYCAST) system (Theophilides *et al*. 2003), the model identifies local WNV risk areas and is based on the hypothesis that West Nile virus propagation occurs in a cycle between birds (hosts) and mosquitoes (vectors). The cycle eventually amplifies, resulting in an increased pool of the virus among birds. Mosquitoes that feed on both birds and humans are then more likely to carry and transmit the virus to humans (Campbell *et al*. 2002). Theophilides *et al*.'s (2003) working hypothesis is that unusually high numbers of crow and blue jay deaths occurring close in space and time signal the presence of an intense amplification cycle and increased risk to humans and that the DYCAST (Theophilides *et al*. 2003) models this amplification process as a continuum in space and time. DYCAST's implementation in New York City in 2001 (Theophilides *et al*. 2003) demonstrated that West Nile virus risk could be identified in a timely and specific way, prior to the onset of human infections. Others have shown that local high dead crow densities precede the occurrence of human WNV infections (Eidson *et al.* 2001, Watson *et al.* 2004). Despite the consensus of observations that bird deaths precede human infections in specific areas, to date, no quantitative evidence has ever been presented that links bird deaths to the spatial and temporal parameters of the amplification process, and the spillover of the virus from avian to human hosts.

Here, we present a retrospective analysis of data of dead birds and human infections that provides this quantitative evidence. These data were collected by the Chicago Department of Health from 30 June to 5 October 2002. The analysis

employs DYCAST (Theophilides *et al.* 2003) modified to use an unconditional Knox methodology that uses a Monte Carlo distribution to test for significance. The results are analysed for predictability beyond random chance using a weighted Kappa analysis for a range of temporal windows selected prior to the date of each human case.

2. Materials and methods

2.1 *Data description*

The data were provided by the Chicago Department of Health and include the location and date of dead bird reports (primarily crows and blue jays, $n=3837$), as called in by the public (followed by office data geocoding at the street level, verification, and cleaning with occasional field verifications), and the location and date of the onset of human West Nile virus infection ($n=215$). The infection of humans was assumed to occur at the place of residence. The analyses were performed over a 0.8 km (half-mile) grid (with 1189 cells) overlaid across the City of Chicago.

2.2 *Analysis*

2.2.1 DYCAST procedure. The data were imported into the DYCAST (Theophilides *et al.* 2003) system and processed for every day between 30 June 2002 and 5 October 2002, (the period of Chicago Health Department, dead-bird surveillance). DYCAST was selected because of its successful implementation in New York City and its prospective and dynamic nature. The DYCAST procedure involves laying a grid across the study area and performing a Knox (1964) test over a spatial domain of 2.4 km (1.5 miles) around each cell centroid and a temporal domain of 21 days prior to the current date. The result of this analysis is a surface showing the probability of non-random space–time interaction of bird deaths. When the probability is lower than 0.1, an infectious process, West Nile virus, is likely to be the cause of the bird deaths. This method should not be confused with kernel density estimation, which measures the number of birds per unit area and not the space-time interaction of bird deaths in a defined spatial and temporal domain. While DYCAST is a geographically continuous process, it results in a statistically discrete risk ($p \leqslant 0.1$) no-risk ($p > 0.1$) surface.

DYCAST was run for the Chicago study area using the same Knox test closeness parameters as set by Theophilides *et al.* (2003) for New York City. These were a (0.4 km 0.25 mile) close-space parameter and 3 days close in time, and were selected from an ecologically constraint range in Theophilides *et al*. (2003). The significance of the space–time interaction was evaluated at the $p \leqslant 0.1$ level to reduce any false negatives. New York City is a similar urban environment with the same mosquito vector, the *Culex pipiens*.

For testing the significance of space–time interaction and the resulting probability, Knox (1963) initially proposed a chi-square test for evaluating the significance of the interaction and then a Poisson test (Knox 1964). Both of these tests require that the data (pairs) being evaluated be part of an independent process. Because the pairs are formed by a finite number of points and share points, this requirement is violated (Knox 1964). Moreover, excess clustering in either the space or time dimension of the data can exacerbate this violation, by resulting in an underestimation of the variance.

Mantel (1967) proposed a solution to the significance test that involved the Monte Carlo switching of the space–time labels of the data points and then ranking the actual number of close space–time pairs to the Monte Carlo distribution. Barton and David (1966) found this to result in an approximate Poisson distribution, but this only applied to that specific case (Williams 1984). However, with heavy clustering in either the space or time dimension, the switching of already-close labels tends to influence the variance of the resulting Monte Carlo distribution. For these reasons, and in a departure from Theophilides *et al.* (2003), significance testing was accomplished by an unconditional Monte Carlo extension of the Knox test method.

For a number of points n found within the spatial domain and temporal domain, random sets of n points were generated within the same domain. For each set, the number of close space–time pairs (st), the number of close space pairs (s) and, the number of close time pairs (t) were counted. Based on the distribution of these random runs, the probability level was assessed as:

$$p = P\{(st \geq ST) \cap (s \geq S) \cap (t \geq T)\}$$

where S, T, and ST are the actual number of points found close in space, time, and both, respectively. This unconditional formulation can be contrasted with that of the traditional Knox test, where:

$$p = P\{(st \geq ST) | [(s \geq S) \cap (t \geq T)]\}$$

For the Monte Carlo simulation, 5000 random distributions were generated for each possible count of birds found within the spatial and temporal domain of a cell centroid. These were defined as the area covered by a 2.4 km (1.5 mile) radius circle and the 21 preceding days, respectively. The actual count of dead birds found within the domain of each cell centroid was used to select the appropriate distribution, and the actual number of close space–time dead bird pairs (as defined by an individual close in space $\leqslant 0.4$ km (0.3 miles) and close in time, 3 days of pairs), was then ranked with respect to that for a random distribution. This resulted in the assignment of each of the 1189 cells with a daily probability of random space–time interaction of dead bird pairs. A cell was identified as 'at-risk' for human West Nile virus infection when its probability was less than or equal to 0.1.

2.2.2 Result evaluation. Evaluation of the results was conducted in two ways. First, we calculated the percentage of human WNV infections that occurred in cells that were shown 'at-risk' in the days prior to the onset of the human illness. Second, we sought to evaluate and test the significance of the overlap of at-risk cells with human cases that occurred beyond chance. In these evaluations, we used the results from modified DYCAST and the location and date of the onset of human cases.

2.2.3 Percent of success. In order to calculate the percentage of success, the location of each human case was overlaid on the grid. Each cell containing a human case was queried to determine if it was at risk. This query was performed for each day starting with 21 days prior and leading up to the date of onset of illness. If the query returned true, risk identification was considered to be successful for that day for that cell. Two histograms were constructed, one showing when, prior to human infection, risk was identified, the other showing the persistence of that risk prior to human infection.

Figure 1 shows a histogram of the number of days, prior to the onset of human illness, on which risk was identified in those areas. The x-axis shows the days prior

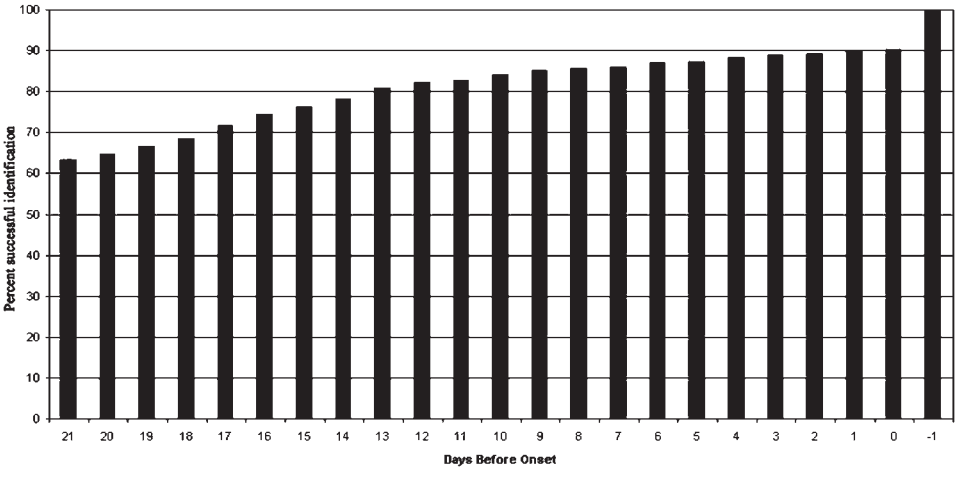

Figure 1. Cumulative histogram of number of days prior to onset of human illness, risk was identified in those areas. *x*-axis: days prior to onset; *y*-axis: cumulative percentage of human cases appearing in cells shown at risk (−1 indicates that risk was not identified by the modified DYCAST).

to onset, and the *y*-axis the cumulative percentage of human cases appearing in cells shown at risk.

Figure 2 shows a cumulative histogram of the number of days on which risk identification was sustained prior to human illness. The *x*-axis shows the number of days on which risk was persistent, and the *y*-axis the cumulative percentage of human cases.

2.2.4 Kappa. The results of percentage success indicate the potential association of dead birds and human risk. However, this association cannot be statistically tested and does not account for successful identification occurring by chance (henceforth called chance agreement). Stated differently, the high sensitivity of the results may have a reciprocal low geographic specificity. In such a case, many more risk cells

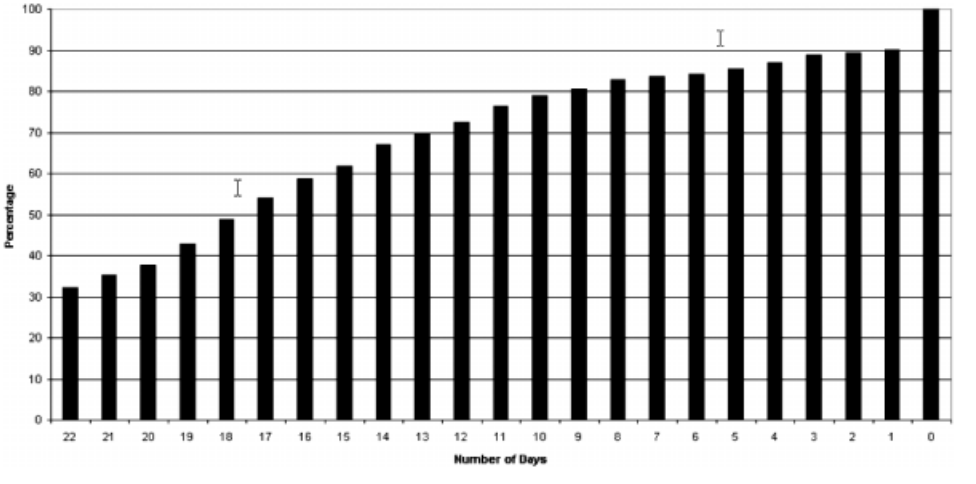

Figure 2. Cumulative histogram of number of days risk identification was sustained prior to human illness. *x*-axis: days risk was persistent; *y*-axis: cumulative percentage of human cases.

would have been identified, increasing the potential that the high sensitivity is the result of the high probability of chance intersection of the human cases with the numerous risk cells, not the efficacy of the model. To control for this and to statistically test the association, we decided to use the kappa index of agreement (or kappa statistic; Cohen 1960). The kappa statistic is used to quantify and test the non-chance agreement between a set of data independently assigned by two raters or methods into nominal classes. In this case, the 'methods' consist of the modified DYCAST procedure and the actual human infections. Each method can classify each grid cell as being at WNV risk (or actual WNV sickness) or at no risk (no WNV sickness) independently from the other. A chi-square statistical test for the significance of the agreement can be performed.

2.2.5 Calculation and scaling of kappa values. The spatial version of the kappa statistic was introduced by Congalton and Mead (1983) and Congalton (1991), and is widely used in Remote Sensing; however, it was never implemented for a space–time database. Here, we present for the first time a methodology for implementation of kappa over space and time. In this methodology, kappa values are calculated for unique combinations of differently sized temporal windows of consecutive days, and lags of given number of days prior to the onset of each human infection. The temporal windows ranged from 1 to 21 days, and the lags ranged from 0 to 17 days prior to onset. An example of a combination of 12 days previously with a 2 day window is shown in figure 3.

The general form of the kappa statistic is defined as:

$$\kappa = \frac{N \sum_{i=1}^{r} x_{ii} - \sum_{i=1}^{r} (x_{i+} * x_{+i})}{N^2 - \sum_{i=1}^{r} (x_{i+} * x_{+i})},$$

where N is the total number of areas considered, and x_{ii}, x_{i+}, x_{+i} are the elements of the matrix shown in table 1, the sum of which amounts to N.

In the spatial and temporal implementation of kappa, a kappa value is calculated for all unique combinations of a range of days prior to onset of illness in humans and a range of temporal windows in order to find the date and duration of maximum non-chance agreement between DYCAST results and human illnesses. The total number of cells for any unique combination of days prior to onset and a

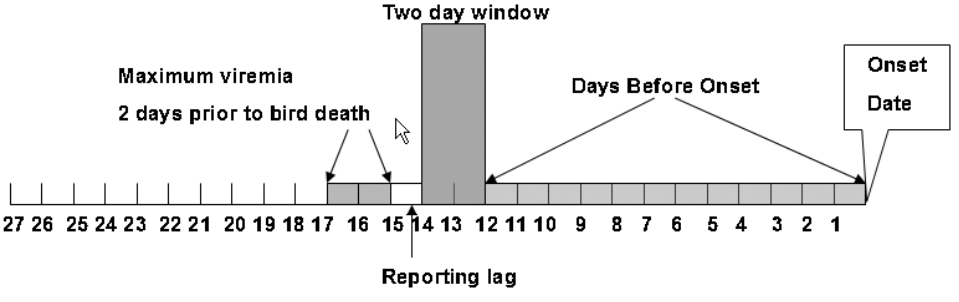

Figure 3. Illustration of temporal windows and days prior to onset and model prediction: most likely time maximum viremia exist in environment.

Table 1. x_{ii}, x_{i+}, and x_{+i} elements of the matrix.

	Rater 1	
Rater 2	Class 1	Class 2
Class 1	x_{11}	x_{12}
Class 2	x_{21}	x_{22}

window is expressed as:

$$N = \sum_{d=30\ \text{June}\ 2002}^{5\ \text{October}\ 2002} G * I$$

where G is equal to 1181, the number cells of the Chicago grid, and I is an indicator function, which can be evaluated as follows:

(1) $I=1$ if, for dates ($d+p$ days) to ($d+p$ days)+($w-1$ days), there is at least one human case, where d is the date, p is the number of days prior to onset, and w is the window size.
(2) $I=0$ otherwise.

The calculation of the kappa values and their respective chi-square test was done over a combination of $p=0$–21 and $w=1$–19.

The parameters for calculating the kappa statistic consist of total possible agreement, expected chance agreement, and observed agreement. The total possible agreement is calculated as the product of the number of human illnesses multiplied by the size of the temporal window. Expected chance agreement is the ratio of at-risk cells to total cells (over the windows) multiplied by total possible agreement. Observed agreement is the sum over all human cases of the number of at risk cells contained within the temporal window overlapping the location of a human case. The agreement for no-risk/no-human-illness cells was calculated in a similar fashion. We calculated kappa values for both classes of agreement and combined them together based on the ratio of total possible agreement in the absence of WNV cells divided by the total possible agreement in presence of WNV cells (the former was far higher than the latter). Whenever the two rating categories are not equally likely, some decision must be made, explicitly or implicitly, as to how to weight agreement in each. The weighting scheme chosen addresses two goals. First, it is based on a first-order approximation to the variance of kappa for each class; that is, it produces the estimate of kappa with the least variance. See Fleiss *et al.* (1969). Second, this combination is also equivalent to the assumption that the cost of a misclassification is directly related to the rarity of an event; Bloch and Kraemer (1988). The results are shown in figures 4 and 5. The significance of the resulting weighted kappa values was tested using a chi-square statistic (CI: 95%).

3. Results

The results show that 14 days or more prior to the onset of illness, risk was identified in 79.14% of 0.162 km^2 (40 acres) cells in which human cases appeared (figure 1). In 84.19% of cells containing human infections, the risk was consistently shown to appear for at least 10 days (figure 2). This means that risk was identified prior to the onset of human cases and existed for many days. In fact, for 76.18% of the cells in which human cases occurred, risk was shown at least 15 days before onset, possibly

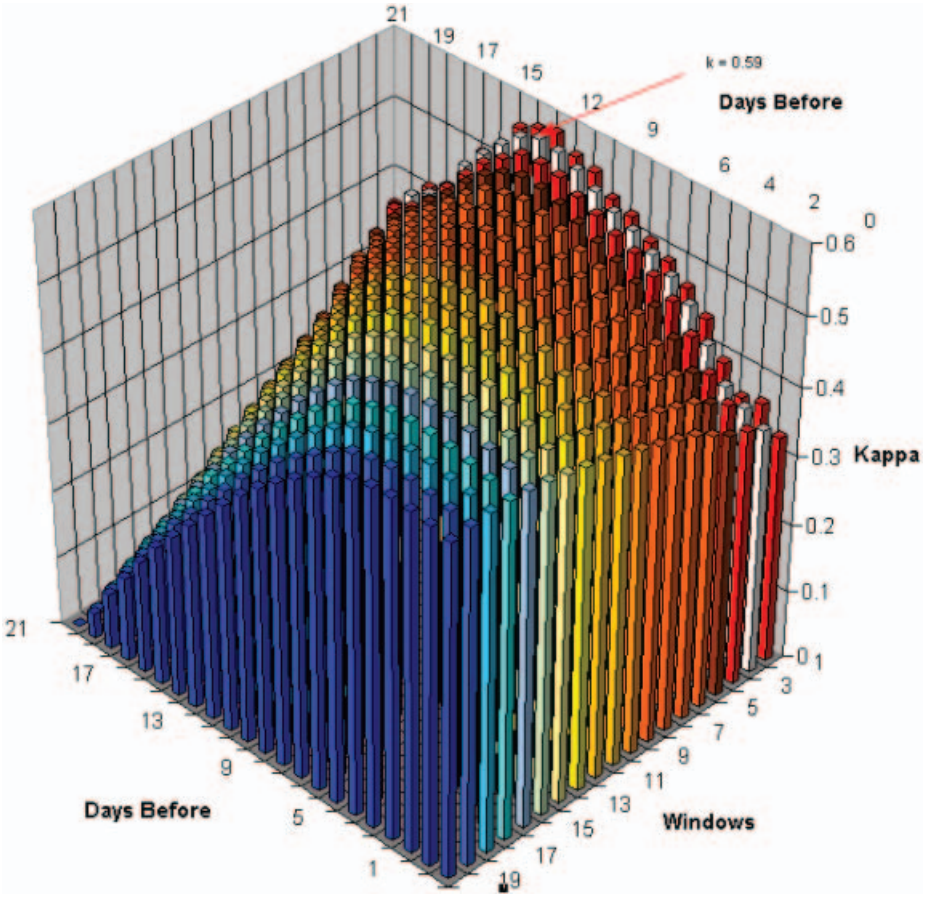

Figure 4. Surface of kappa values for varying combinations of days prior to illness and window size. *x*-axis: days prior to onset; *y*-axis: windows; *z*-axis: kappa values.

before the humans were bitten by mosquitoes, assuming that the range of incubation is 3–15 days (Olejnik 1952).

Figure 4 shows a surface created from kappa values, which indicate non-chance agreement between human cases and close space–time bird deaths, for a range of different combinations of number of days prior to the onset of human illness (henceforth called days prior) and window sizes (figure 3). All kappa values of more than 0.025 were statistically significant (probably due to a large number of samples) and clearly showing that there is a statistically significant spatio-temporal relationship between non-random space–time interaction of bird deaths and human illnesses for a range of combinations of days prior to the onset of illness and window sizes. The strength of this relationship varies with days prior to onset and window size.

The variation in the strength of this relationship is more clearly seen if one considers the combinations of window size and days prior that have a non-chance agreement of over 50% (kappa $\geqslant$0.5, figure 5). These combinations are bound by an upper and lower limit of days prior to onset and are characterized by an increase in the kappa value to a maximum followed by drop-off as the day of onset of human

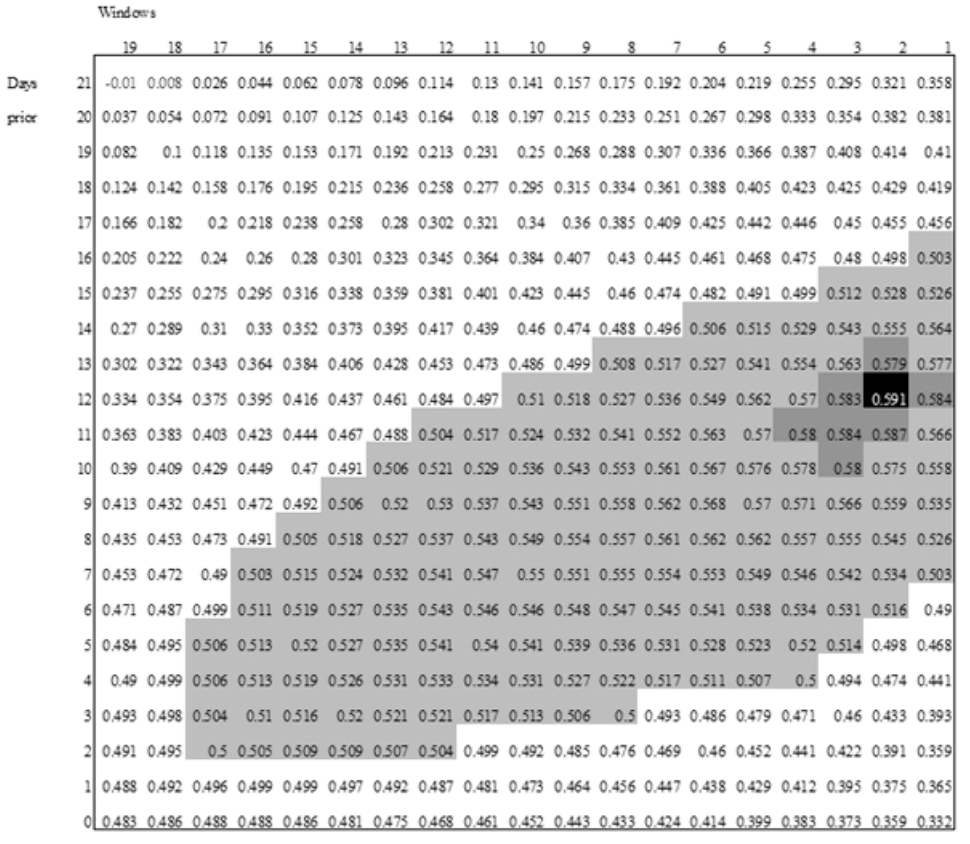

Days prior	Windows 19	18	17	16	15	14	13	12	11	10	9	8	7	6	5	4	3	2	1
21	-0.01	0.008	0.026	0.044	0.062	0.078	0.096	0.114	0.13	0.141	0.157	0.175	0.192	0.204	0.219	0.255	0.295	0.321	0.358
20	0.037	0.054	0.072	0.091	0.107	0.125	0.143	0.164	0.18	0.197	0.215	0.233	0.251	0.267	0.298	0.333	0.354	0.382	0.381
19	0.082	0.1	0.118	0.135	0.153	0.171	0.192	0.213	0.231	0.25	0.268	0.288	0.307	0.336	0.366	0.387	0.408	0.414	0.41
18	0.124	0.142	0.158	0.176	0.195	0.215	0.236	0.258	0.277	0.295	0.315	0.334	0.361	0.388	0.405	0.423	0.425	0.429	0.419
17	0.166	0.182	0.2	0.218	0.238	0.258	0.28	0.302	0.321	0.34	0.36	0.385	0.409	0.425	0.442	0.446	0.45	0.455	0.456
16	0.205	0.222	0.24	0.26	0.28	0.301	0.323	0.345	0.364	0.384	0.407	0.43	0.445	0.461	0.468	0.475	0.48	0.498	0.503
15	0.237	0.255	0.275	0.295	0.316	0.338	0.359	0.381	0.401	0.423	0.445	0.46	0.474	0.482	0.491	0.499	0.512	0.528	0.526
14	0.27	0.289	0.31	0.33	0.352	0.373	0.395	0.417	0.439	0.46	0.474	0.488	0.496	0.506	0.515	0.529	0.543	0.555	0.564
13	0.302	0.322	0.343	0.364	0.384	0.406	0.428	0.453	0.473	0.486	0.499	0.508	0.517	0.527	0.541	0.554	0.563	0.579	0.577
12	0.334	0.354	0.375	0.395	0.416	0.437	0.461	0.484	0.497	0.51	0.518	0.527	0.536	0.549	0.562	0.57	0.583	0.591	0.584
11	0.363	0.383	0.403	0.423	0.444	0.467	0.488	0.504	0.517	0.524	0.532	0.541	0.552	0.563	0.57	0.58	0.584	0.587	0.566
10	0.39	0.409	0.429	0.449	0.47	0.491	0.506	0.521	0.529	0.536	0.543	0.553	0.561	0.567	0.576	0.578	0.58	0.575	0.558
9	0.413	0.432	0.451	0.472	0.492	0.506	0.52	0.53	0.537	0.543	0.551	0.558	0.562	0.568	0.57	0.571	0.566	0.559	0.535
8	0.435	0.453	0.473	0.491	0.505	0.518	0.527	0.537	0.543	0.549	0.554	0.557	0.561	0.562	0.562	0.557	0.555	0.545	0.526
7	0.453	0.472	0.49	0.503	0.515	0.524	0.532	0.541	0.547	0.55	0.551	0.555	0.554	0.553	0.549	0.546	0.542	0.534	0.503
6	0.471	0.487	0.499	0.511	0.519	0.527	0.535	0.543	0.546	0.546	0.548	0.547	0.545	0.541	0.538	0.534	0.531	0.516	0.49
5	0.484	0.495	0.506	0.513	0.52	0.527	0.535	0.541	0.54	0.541	0.539	0.536	0.531	0.528	0.523	0.52	0.514	0.498	0.468
4	0.49	0.499	0.506	0.513	0.519	0.526	0.531	0.533	0.534	0.531	0.527	0.522	0.517	0.511	0.507	0.5	0.494	0.474	0.441
3	0.493	0.498	0.504	0.51	0.516	0.52	0.521	0.521	0.517	0.513	0.506	0.5	0.493	0.486	0.479	0.471	0.46	0.433	0.393
2	0.491	0.495	0.5	0.505	0.509	0.509	0.507	0.504	0.499	0.492	0.485	0.476	0.469	0.46	0.452	0.441	0.422	0.391	0.359
1	0.488	0.492	0.496	0.499	0.499	0.497	0.492	0.487	0.481	0.473	0.464	0.456	0.447	0.438	0.429	0.412	0.395	0.375	0.365
0	0.483	0.486	0.488	0.488	0.486	0.481	0.475	0.468	0.461	0.452	0.443	0.433	0.424	0.414	0.399	0.383	0.373	0.359	0.332

Figure 5. Kappa agreement results for varying window size and days prior. Kappa values of higher than 0.5 are shown in grey squares. The peak value is shown in black.

illness approaches (figures 4 and 5). The highest kappa values in descending order occur for windows of 2, 3, 1, and 4 days, and are consistent with the fact that viremia—sufficient to infect mosquitoes—in crows and blue jays lasts for 1–4 days (Komar *et al.* 2003). The maximum kappa value of 0.59 occurs at 12 days prior with a 2 day window (figures 3 and 4). Adjusting for a 1 day reporting lag (by the public), the maximum non-chance agreement occurs during days 13 and 14 prior to the onset of illness. Based on this and the fact that peak viremia occurs 1–2 days prior to bird deaths (Komar *et al.* 2003), we can deduce that the maximum pool of virus in the avian hosts that die occurs approximately 15–16 days prior to the onset of human illness. Assuming that mosquitoes constantly feed on all available birds, this peak die-off also represents the peak of the amplification cycle and the time the maximum pool of the virus circulates in the entire avian population. Hence, it is the most likely time that mosquitoes that bridge the virus to humans became infected. This is consistent with the mean of the extrinsic incubation period in mosquitoes of 4–12 days (Dohm *et al.* 2002) and the intrinsic incubation period in humans. Human intrinsic incubation periods are reported to range from 2–6 days (Goldblum *et al.* 1954) to 3–15 days (Olejnik 1952), though the exact range is still unknown (Petersen and Marfin 2002). The temporal relationship between the model results (figure 3) and the epidemiological progression of infection (figure 5) is shown by comparing figure 3 with figure 6.

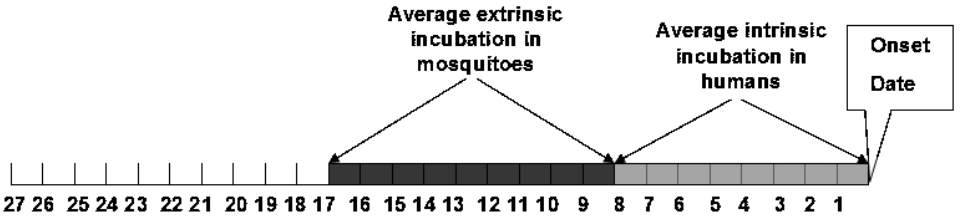

Figure 6. Time: mosquito infection to onset date of human infection.

The period of likely human infection is preceded by an increase in the kappa value to a maximum and coincides with a downward trend of the kappa values that leads to a drop of more than 30% by day 4 prior (figures 4 and 5, 2 day window). This is a statistical manifestation of the temporal characteristics of the amplification cycle. The downward trend in kappa is a result of fewer birds dying close in space and time as we approach the onset of human illness. We believe that the decreased dead bird activity is due to a localized reduction in the bird population. Because of this reduction, mosquitoes (that have increased significantly in numbers by now due to peak availability in blood meals) that feed on both birds and mammals (Fonseca *et al.* 2004) are more likely to turn to dead-end hosts like humans and other mammals for blood meals (the so-called 'spillover' effect). These results suggest that by the time a human develops symptoms of WNV disease, the amplification cycle has been disrupted in that local area due to a die-off of a substantial number of competent hosts.

4. Conclusions

Through the use of both geostatistical and spatially analytic techniques, we have provided evidence that corvid deaths are an integral part of the local West Nile virus amplification cycle and that this cycle peaks 15–16 days prior to the onset of human illness, a period that is consistent with the epidemiology of the virus transmission from bird to mosquito to human in the same approximate time frame. This peak is followed by a substantial reduction in the amplification activity, as shown by the dramatic reduction in the kappa values as the day of human infection draws near. The implication for remediation is that by the time a human has become sick in an area, the risk decreases as the amplification process is subsiding, and spraying of adulticide may have little or no effect.

Furthermore, we have demonstrated that the unconditional extension of the Knox test is a more appropriate space–time measure when interdependence of points of the Knox data pairs is of concern. The approximate parametric and conditional Monte Carlo significance tests that suffer from over- or underestimation of the variance due to spatial autocorrelation and lack of pair independence were replaced by an unconditional Monte Carlo test. This test uses random independently distributed uniform sets of points in the space–time domain that reflect the actual distribution of the close space–time pairs and their marginal individual space and time distributions. This allows the probability of the margins to be fixed and included in the test rather than allowing them to bias the results. On a more practical matter, the unconditional extension of the Knox will capture instances where all pairs are close in space and time as an epidemic outbreak, whereas the original Knox (1963, 1964) test may not.

In addition, the unique implementation of the space–time kappa measure is effective in evaluating agreement in spatially explicit dynamic phenomena. While in Remote Sensing the kappa coefficient (Congalton 1991) is routinely used in its spatial form, this is the first time it was applied in a space–time domain for identifying a biological relationship. The use of varying size temporal windows and days prior helped isolate the period of maximum amplification activity, and the gradual increase and decrease in the resulting surface of kappa values verify that this is the result of a physical/biological process.

What is not known is whether this decrease in activity is because of significant bird die-offs, bird migration, or a combination of both. However, there is now evidence that crows are dying of the West Nile virus in significant numbers (Yaremych *et al.* 2004), at least in Illinois. In the City of Chicago, corvids populations were reduced by 82% as a result of the 2002 epidemic (Watson *et al.* 2004), while West Nile virus infections in humans in 2003 were less than 5% of the 2002 human infections. In addition, the amplification process and human infections are highly dependent on the predilection of the species of mosquitoes to feed on birds or humans, and their feeding behaviour needs to be studied further at the local level; however, there is evidence that *Culex pipiens* is capable of feeding on both humans and birds (Fonseca *et al.* 2004).

We caution that the findings of this study should not be interpreted as the only process operating behind West Nile virus human infections globally. West Nile virus is a newly introduced agent in the United States, and this could be viewed as evidence of a process operating on a naïve amplification host population.

Acknowledgements

The authors would like to thank the Centers for Disease Control making this research possible. We would also like to acknowledge Dr Dickson Despommier (School of Public Health, Columbia University), for his assistance on West Nile virus transmission dynamics, and thank Dr Nicholas Komar (CDC) and John-Paul Mutebi (Chicago Department of Health), for reviewing and providing thoughtful critiques to this manuscript.

References

Barton, D.W. and David, F.N., 1966, The random intersection of two graphs. In: Research papers in Statistics, F.N. David (Ed.) (New York: Wiley).

Bloch, D.A. and Kraemer, H.C., 1988, Kappa coefficients in epidemiology: an appraisal of a reappaisal. *Journal of Clinical Epidemiology*, **41**, pp. 959–968.

Campbell, G.L., Marfin, A.A., Lanciotti, R.S. and Gubler, D.J., 2002, West Nile virus. *Lancet Infectious Diseases*, **2**, pp. 519–529.

Cohen, J., 1960, A coefficient of agreement for nominal scales. *Educational and Psychological Measurement*, **20**, pp. 37–46.

Congalton, R.G., 1991, A review of assessing the accuracy of classifications of remotely sensed data. *Remote Sensing and the Environment*, **37**, pp. 35–46.

Congalton, R.G. and Mead, R.A., 1983, A quantitative method to test for consistency and correctness in photointerpretation. *Photogrammetric Engineering and Remote Sensing*, **49**(1), pp. 69–74.

Dohm, D.J., O'Guinn, M.L. and Turell, M.J., 2002, Effect of environmental temperature on the ability of *Culex pipiens* (Diptera: Culicidae) to transmit West Nile virus. *Journal of Medical Entomology*, **39**, pp. 221–225.

EIDSON, M., KRAMER, L., STONE, W., HAGIWARA, Y. and SCHMIT, K., The New York State West Nile Virus Avian Surveillance Team 2001, Dead bird surveillance as an early warning system for West Nile virus. *Emerging Infectious Diseases*, **7**, pp. 631–635.

FLEISS, J.L., COHEN, J. and EVERITT, B.S., 1969, Large sample standard errors of kappa and weighted kappa. *Psychological Bulletin*, **72**, pp. 323–327.

FONSECA, D.M., KEYGHOBADI, N., MALCOM, C.M., SCHAFFNER, F., MOTOYOSHI, M., FLEISCHER, R.C. and WILKERSON, R.C., 2004, Emerging vectors in the *Culex pipiens* Complex. *Science*, **303**, pp. 1535–1538.

GOLDBLUM, N., STERK, V.V. and PADERSKI, B., 1954, West Nile fever: The clinical features of the disease and the isolation of West Nile virus from the blood of nine human cases. *American Journal of Hygiene*, **59**, pp. 89–103.

HAYES, C.G., 2001, West Nile Virus: Uganda, 1937, to New York City, 1999. *Annals of the New York Academy of Sciences*, **951**, pp. 25–37.

KNOX, G.E., 1963, Detection of low intensity epidemicity. Application to cleft lip and palate. *British Journal of Preventative Social Medicine*, **17**, pp. 121–7.

KNOX, G.E., 1964, The detection of space–time interactions. *Journal of the Royal Statistical Society (C)*, **13**, pp. 25–29.

KOMAR, N., LANGEVIN, S., HINTEN, S., NEMETH, N., EDWARDS, E., HETTLER, D., DAVIS, B., BOWEN, R. and BUNNING, M., 2003, Experimental infection of North American birds with the New York 1999 strain of West Nile virus. *Emerging Infectious Diseases*, **9**, pp. 311–322.

KULASEKERA, V., KRAMER, L., NASCI, R.S., MOSTASHARI, F., CHERRY, B., TROCK, S.C., GLASER, S. and MILLER, J.R., 2001, West Nile Virus infection in mosquitoes, birds, horses, and humans, Staten Island, New York, 2000. *Emerging Infectious Diseases*, **7**, pp. 722–725.

KULLDORFF, M., 1997, A spatial scan statistic. *Communications in Statistics: Theory and Methods*, **26**, pp. 1481–1496.

LANCIOTTI, R.S., ROEHRIG, J.T., DEUBEL, V., SMITH, J., PARKER, M., STEELE, K., CRISE, B., VOLPE, K.E., CRABTREE, M.B., SCHERRET, J.H., HALL, R.A., MACKENZIE, J.S., CROPP, C.B., PANIGRAHY, B., OSTLUND, E., SCHMITT, B., MALKINSON, M., BANET, C., WEISSMAN, J., KOMAR, N., SAVAGE, H.M., STONE, W., MCNAMARA, T. and GUBLER, D.J., 1999, Origin of the West Nile virus responsible for an outbreak of encephalitis in the northeastern U.S. *Science*, **286**, pp. 2333–2337.

MANTEL, N., 1967, The detection clustering and a generalized regression approach. *Cancer Research*, **27**, pp. 209–220.

MCLEAN, R.G., UBICO, S.R., DOCHERTY, D.E., HANSEN, W.R., SILEO, L. and MCNAMARA, T., 2001, West Nile virus transmission and ecology in birds. *Annals of the New York Academy of Science*, **951**, pp. 54–57.

MOSTASHARI, F., KULLDORFF, M., HARTMAN, J.J., MILLER, J.R. and KULASEKERA, V., 2003, Dead bird clustering: A potential early warning system for West Nile virus activity. *Emerging Infectious Diseases*, **9**, pp. 641–646.

NASH, D., MOSTASHARI, F., FINE, A., MILLER, J., O'LEARY, D., MURRAY, K., HUANG, A., ROSENBERG, A., GREENBERG, A., SHERMAN, M., WONG, S. and LAYTON, M. and the West Nile Outbreak Response Working Group, 2001, The outbreak of West Nile virus infection in the New York City area in 1999. *New England Journal of Medicine*, **344**, pp. 1807–1814.

OLEJNIK, E., 1952, Infectious adenitis transmitted by Cx. molestus. *Bulletin of the Research Council of Israel*, **2**, pp. 210–211.

PETERSEN, L. and MARFIN, A., 2002, West Nile virus: a primer for the clinician. *Annals of Internal Medicine*, **137**, pp. 173–179.

ROGERSON, P.A., 2001, Monitoring point patterns for the development of space–time clusters. *Journal of the Royal Statistical Society* (A), **164**, pp. 87–96.

SMITHBURN, K.C., HUGHES, T.P., BURKE, A.W. and PAUL, J.H., 1940, A neurotropic virus isolated from the blood of a native of Uganda. *American Journal of Tropical Medicine and Hygiene*, **20**, pp. 471–492.

THEOPHILIDES, C.N., AHEARN, S.C., GRADY, S. and MERLINO, M., 2003, Identifying West Nile Virus risk areas: The dynamic continuous-area space–time system. *American Journal of Epidemiology*, **157**, pp. 843–854.

WATSON, J.T., JONES, R.C., GIBBS, K. and PAUL, W., 2004, Dead crow reports and human West Nile virus cases, Chicago, 2002. *Emerging Infectious Diseases*, **10**, pp. 938–940.

WILLIAMS, G.W., 1984, Time–space clustering of disease. In *Statistical Methods for Cancer Studies*, R.G. Cornell (Eds.), pp. 167–227 (New York: Marcel Dekker).

YAREMYCH, S.A., WARNER, R.E., MANKIN, P.C., BRAWN, J.D., RAIM, A. and NOVAK, R., 2004, West Nile virus and high death rate in American Crows. *Emerging Infectious Diseases*, **10**, pp. 709–711.